

Published in final edited form as:

Clin Cancer Res. 2018 October 15; 24(20): 4988–4996. doi:10.1158/1078-0432.CCR-18-0786.

Molecular Imaging of Radiolabeled Bispecific T-cell Engager ⁸⁹Zr-AMG211 Targeting CEA-positive Tumors

Stijn J.H. Waaijer¹, Frank J. Warnders², Sabine Stienen³, Matthias Friedrich³, Alexander Sternjak³, H. Kam Cheung⁴, Anton G.T. Terwisscha van Scheltinga², Carolien P. Schröder¹, Elisabeth G.E. de Vries¹, and Marjolijn N. Lub-de Hooge²

¹Department of Medical Oncology, University Medical Center Groningen, Groningen, the Netherlands ²Department of Clinical Pharmacy and Pharmacology, University Medical Center Groningen, Groningen, the Netherlands ³Amgen Research Munich GmbH, Munich, Germany ⁴Amgen Inc, Thousand Oaks, CA

Abstract

Background—AMG 211, a bispecific T-cell engager (BiTE) antibody construct, targets carcinoembryonic antigen (CEA) and the CD3 epsilon subunit of the human T-cell receptor. AMG 211 was labeled with zirconium-89 (⁸⁹Zr) or fluorescent dye to evaluate the tumor targeting properties.

Experimental Design—⁸⁹Zr-AMG211 was administered to mice bearing CEA-positive xenograft tumors of LS174T colorectal adenocarcinoma or BT474 breast cancer cells, as well as CEA-negative HL-60 promyelocytic leukemia xenografts. Biodistribution studies with 2–10 µg ⁸⁹Zr-AMG211 supplemented with unlabeled AMG 211 up to 500 µg protein dose were performed. A BiTE[®] that does not bind CEA, ⁸⁹Zr-Mec14, served as a negative control. ⁸⁹Zr-AMG211 integrity was determined in tumor lysates *ex vivo*. Intratumoral distribution was studied with IRDye800CW-AMG211. Moreover, ⁸⁹Zr-AMG211 was manufactured according to Good Manufacturing Practice (GMP) guidelines for clinical trial NCT02760199.

Results—⁸⁹Zr-AMG211 demonstrated dose-dependent tumor uptake at 6 hours. The highest tumor uptake was observed with 2 µg dose, and the lowest tumor uptake was observed with 500 µg dose. After 24 hours, higher uptake of 10 µg ⁸⁹Zr-AMG211 occurred in CEA-positive xenografts,

Corresponding author: M.N. Lub-de Hooge, PharmD, PhD, Department of Clinical Pharmacy and Pharmacology, University Medical Center Groningen, University of Groningen, PO Box 30.001, 9700 RB Groningen, The Netherlands. +31 50 36 14071 (phone); +31 50 36 14087 (fax); m.n.de.hooge@umcg.nl.

Authors' Contributions

Conception and design: S.J.H. Waaijer, F.J. Warnders, S. Stienen, M. Friedrich, A. Sternjak, M.N. Lub-de Hooge, H.K. Cheung, A.G.T. Terwisscha van Scheltinga, E.G.E. de Vries

Development of methodology: F.J. Warnders, M.N. Lub-de Hooge, M. Friedrich, A. Sternjak, A.G.T. Terwisscha van Scheltinga

Acquisition of data (provided animals, acquired and managed patients, provided facilities, etc.): S.J.H. Waaijer, F.J. Warnders

Analysis and interpretation of data (e.g., statistical analysis, biostatistics, computational analysis): S.J.H. Waaijer, F.J. Warnders, M.N. Lub-de Hooge, H.K. Cheung, E.G.E. de Vries

Writing, review, and/or revision of the manuscript: S.J.H. Waaijer, F.J. Warnders, S. Stienen, M. Friedrich, A. Sternjak, M.N. Lub-de Hooge, H.K. Cheung, A.G.T. Terwisscha van Scheltinga, C.P. Schröder, E.G.E. de Vries

Administrative, technical or material support: S.J.H. Waaijer, M. Friedrich, A. Sternjak

Study supervision: M.N. Lub-de Hooge, S. Stienen, H.K. Cheung, C.P. Schröder, E.G.E. de Vries

compared to CEA-negative xenografts. Although the blood half-life of ^{89}Zr -AMG211 was ~1 hour, tumor retention persisted for at least 24 hours. ^{89}Zr -Mec14 showed no tumor accumulation beyond background level. *Ex vivo* autoradiography revealed time-dependent disintegration of ^{89}Zr -AMG211. 800CW-AMG211 was specifically localized in CEA-expressing viable tumor tissue. GMP-manufactured ^{89}Zr -AMG211 fulfilled release specifications.

Conclusions— ^{89}Zr -AMG211 showed dose-dependent CEA-specific tumor targeting and localization in viable tumor tissue. Our data enabled its use to clinically evaluate AMG 211 *in vivo* behavior.

Keywords

Bispecific T cell engager; PET imaging; drug development

Introduction

Recent advances in immuno-oncology and approval of several immune-enhancing cancer therapies have led to great enthusiasm and exploration of various approaches to target cytotoxic T cells specifically to the tumor for killing. Novel therapeutic approaches such as bispecific T-cell engager (BiTE) antibody constructs are engineered by combining two single-chain variable fragment (scFv) domains of two different antibodies (1). One scFv domain is directed against the epsilon chain of CD3 (CD3 ϵ), a part of the T-cell receptor complex, and the other domain is directed against a tumor-associated antigen. Connected by a flexible linker, the two single chain Fv regions have a combined molecular weight of approximately 54 kilodalton (kDa). Simultaneous binding of both domains to their targets forms a bridge between a tumor cell and a T cell eventually resulting in the formation of a cytolytic synapse, followed by killing of the tumor cell via perforin and granzyme B mediated lysis (2).

The first BiTE antibody construct approved was the CD19-targeting molecule blinatumomab (Blinicyto[®]). It is used to treat patients with Philadelphia chromosome-negative relapsed or refractory B-cell precursor acute lymphoblastic leukemia. Other BiTE antibody constructs that have been explored in phase I trials include AMG 110 (MT110; solitomab), AMG 211 (MEDI-565; MT111), and BAY2010112 for targeting of epithelial cell adhesion molecule (EpCAM), carcinoembryonic antigen (CEA), and prostate-specific membrane antigen (PSMA) expressing solid tumors, respectively (3, 4).

For CEA overexpressing solid tumors, AMG 211 is a potential interesting new BiTE antibody construct. *In vitro*, AMG 211 lyses explants of metastatic colorectal cancer cells of patients who progressed on chemotherapy (5). In addition, immune checkpoint inhibition combined with AMG 211 resulted in a more potent cytotoxicity towards CEA-positive tumor cells *in vitro* (6). Although T-cell inhibition could not be fully reversed in T cells previously exposed to AMG 211, prior treatment with checkpoint inhibition is a potential combination strategy. AMG 211 mediated cytotoxicity is independent of the presence of soluble CEA, CEA splice variants, CEA single-nucleotide polymorphisms or commonly found oncogenic mutations in colorectal adenocarcinomas (7–9). A first-in-human study with an intermittent administration regimen of 3-hour continuous intravenous infusion once

a day, on days 1 through 5, in 28-day cycles with AMG 211, showed a maximum tolerated dose of 5 mg with linear and dose-proportional pharmacokinetics (4). In this study, the best tumor response was stable disease, which was observed in 28% of the patients. For BiTE antibody constructs to be effective in solid tumors, the molecule should be able to penetrate tumors and be present in sufficient amounts to maintain continuous exposure, and the tumor should have sufficient T-cell infiltration. To establish prolonged steady state exposure, continuous intravenous administration of AMG 211 over 7 to 28 days was tested in a recently completed phase I trial (NCT02291614).

Strikingly, little is known concerning whole body distribution and tumor targeting of BiTE antibody constructs in cancer patients. Therefore, to enable clinical exploration of the *in vivo* properties of BiTE antibody constructs, we developed ^{89}Zr -AMG211 for testing in preclinical mouse models. With molecular imaging, information on whole-body drug distribution, tumor targeting and tissue pharmacokinetics can be obtained non-invasively. In this study, ^{89}Zr -AMG211 microPET imaging was also complemented with *ex vivo* biodistribution and tracer integrity analysis. In addition, AMG 211 was labeled with the near-infrared fluorescent dye 800CW to study intratumoral distribution. Finally, we manufactured ^{89}Zr -AMG211 according to Good Manufacturing Practice (GMP) guidelines that enabled clinical evaluation.

Materials and Methods

BiTE antibody constructs and cell lines

The BiTE antibody constructs AMG 211 and Mec14 were provided by Amgen, Inc. AMG 211, which binds human CD3e and human CEA, was formulated in 30 mM sodium citrate, 75 mM L-lysine hydrochloride, 6.5% mM trehalose dihydrate, and 0.02% (w/v) plant derived polysorbate 80; pH 6.0. Mec14, which binds human CD3e and the herbicide mecoprop, was formulated in 10 mM citrate, 75 mM L-lysine hydrochloride, 4% (w/v) trehalose dihydrate, and 0.03% (w/v) polysorbate 80, pH 7.0. AMG 211 equilibrium dissociation constants were estimated as 5.5 ± 2.2 nM and 310 ± 67 nM for human CEA and CD3e, respectively (7). The molecular weight of the BiTE antibody constructs is approximately 54 kDa. The human colorectal cancer cell line LS174T (CEA+), human breast cancer cell line BT474 (CEA+), and promyelocytic leukemia cell line HL-60 (CEA-) were used. All cell lines were obtained from American Type Culture Collection and confirmed to be negative for microbial contamination. Cell lines were authenticated by BaseClear using short tandem repeat profiling. This was repeated once a cell line has been passaged for more than 6 months after previous short tandem repeat profiling. BT474 and HL-60 were routinely cultured in RPMI-1640 medium (Invitrogen) containing 10% fetal calf serum (Bodinco BV). LS174T cells were cultured in Dulbecco's Modified Eagle's Medium with high glucose (Invitrogen) supplemented with 10% fetal calf serum. All cells were cultured under humidified conditions at 37°C with 5% CO₂.

Flow cytometry

CEA expression by LS174T, BT474, and HL-60 cells was measured using a BD Accuri™ C6 flow cytometer (BD Biosciences) as described earlier (10). In short, cells were incubated

for 1 hour at 4 °C with either 20 µg/mL mouse anti-human CEACAM5 antibody (Santa Cruz; sc-23928) or mouse IgG1 (Dako). After washing, cells were incubated for 1 hour at 4 °C with goat anti-mouse phycoerythrin secondary antibody (Southern Biotech). After final washing, expression was assessed and calculated as mean fluorescent intensity expressed as percentage of LS174T signal.

Conjugation and labeling of AMG 211 and Mec14

BiTE antibody constructs AMG 211 and Mec14 were purified against NaCl 0.9% (Braun) using a Vivspin-2 10 kDa polyethersulfone filter (Sartorius). Next, *N*-succinyl-desferrioxamine-B-tertrafluorphenol (*N*-sucDf-TFP; ABX) was conjugated to BiTE[®] antibody constructs in a 4-fold molar excess, as described earlier (11). After PD-10 desalting column (GE Healthcare) purification, conjugated BiTE antibody constructs were stored at -80 °C. On the day of labeling with ⁸⁹Zr-oxalate (PerkinElmer), *N*-sucDf conjugated BiTE[®] antibody constructs were thawed and labeled with a maximum specific activity of 500 MBq/mg. For conjugating IRDye 800CW to AMG 211 and 680RD to Mec14 (LI-COR Biosciences), purified BiTE antibody constructs were reacted with a 3-fold molar excess of IRDye *N*-hydroxysuccinimide ester as described earlier (12).

Quality control of ⁸⁹Zr-AMG211 and ⁸⁹Zr-Mec14

Size exclusion high performance liquid chromatography was used to assess aggregation and fragmentation of radiolabeled or fluorescently labeled AMG 211 and Mec14, as described previously (10). Protein concentration was determined by ultraviolet-visible spectrophotometry (Cary 60; Agilent).

Immunoreactivity of ⁸⁹Zr-AMG211 towards CEA was tested in a competition assay with unlabeled AMG 211. Recombinant human CEACAM5 (11077-H08H; Sino Biologicals Inc.) was used as target antigen. CEACAM5 protein was diluted in 0.05 M Na₂CO₃ (pH 9.6) to a concentration of 0.5 µg/mL and 100 µL was coated to Nunc-Immuno BreakApart ELISA plates (NUNC) at 4°C overnight. Next day, wells were blocked using 1% milk powder in 0.05% polysorbate 20 (Sigma-Aldrich)/PBS (140 mM NaCl, 9 mM Na₂HPO₄, 1.3 mM NaH₂PO₄, pH = 7.4, UMCG). After blocking, wells were washed three times with 0.05% polysorbate 20/PBS. ⁸⁹Zr-AMG211 and AMG 211 were mixed and diluted in PBS to result in a fixed concentration of 185 nM ⁸⁹Zr-AMG211 and varying concentrations of unlabeled AMG 211, ranging from 93 pM to 32 µM. These samples were added to the wells and incubated for 2 hours. Samples were washed with 0.05% polysorbate 20 in PBS and ⁸⁹Zr-AMG211 bound to the CEA-coated wells were measured for radioactivity. CEA binding was expressed as percentage radioactivity bound to CEA-coated wells corrected for non-specific binding to uncoated wells. The average amount of CEA bound ⁸⁹Zr-AMG211 at the lowest competing dose of non-radiolabeled AMG 211 was set at 100%. The percentages were plotted against the log-values of AMG 211 concentration using Prism software (GraphPad, Prism 5). The concentration that resulted in 50% inhibition of the maximum binding was calculated. Immunoreactivity was calculated by dividing the half maximal inhibitory concentration (IC₅₀) by added concentration of ⁸⁹Zr-AMG211 (185 nM).

Internalization of ^{89}Zr -AMG211

Internalization of ^{89}Zr -AMG211 was assessed as described earlier (10). In short, 10^6 LS174T cells were incubated with 50 ng (0.93 pmol) ^{89}Zr -AMG211 for 1 hour at 4 °C, followed by incubation for 1, 2 or 4 hours at 4 °C or 37 °C in culture medium. Cells were subsequently stripped using a stripping buffer (0.05 M glycine, 0.1 M NaCl, pH 2.8). Radioactivity of the stripped cell pellet was measured in a calibrated well-type γ -counter (LKB instruments) and expressed as percentage of cell associated activity.

Animal experiments

All animal experiments were approved by the Institutional Animal Care and Use Committee of the University of Groningen. Six to 8 weeks old male nude BALB/c mice (BALB/cOlaHsd-*Foxn1*^{nu}, Harlan) were allowed to acclimate for 1 week. For xenograft development, 2×10^6 LS174T cells in 0.1 mL PBS were subcutaneously injected, for BT474 and HL-60 xenografts, respectively 5×10^6 and 2×10^6 cells in 1:1 ratio of medium and Matrigel™ (BD Biosciences; 0.3 mL) were subcutaneously injected. BT474 inoculated mice received 1 day prior to tumor inoculation a 17 β -estradiol pellet (0.18 mg, 90-day release; Innovative Research of America). Tumor growth was assessed by caliper measurements. Penile vein tracer injection was performed when tumors reached a size of 200 mm³. This was reached for LS174T in 11 days, for HL-60 in 2 weeks, and for BT474 in 4 weeks. Anesthesia was performed with isoflurane/medical air inhalation (5% induction, 2.5% maintenance).

In vivo microPET imaging and *ex vivo* biodistribution

In consecutive experiments, we studied dose and time dependency of biodistribution and tumor uptake, specificity of tumor uptake, and variation in uptake in different CEA-expressing tumor models. Tumor uptake of ^{89}Zr -AMG211 and ^{89}Zr -Mec14 (negative control) was analyzed over time. MicroPET scanning was performed at 0.5, 3, 6, and 24 hours after injection with 5 MBq (10 μg ; 0.19 nmol) of tracer. Mice were sacrificed 24 hours after tracer injection and thereafter *ex vivo* biodistribution was performed.

To study dose dependent tumor uptake of ^{89}Zr -AMG211, LS174T xenograft bearing mice were injected with a protein dose of 2 (0.04 nmol; $n = 6$), 10 (0.19 nmol; $n = 6$), 50 (0.93 nmol; $n = 6$), 100 (1.85 nmol; $n = 6$), and 500 μg (9.26 nmol; $n = 3$) of ^{89}Zr -AMG211 (1 MBq), sacrificed at 6 hours after injection followed by *ex vivo* biodistribution. Doses higher than 10 μg (0.19 nmol) were supplemented with non-radiolabeled AMG 211.

Non-specific uptake was studied in two groups of mice bearing LS174T xenografts. Either 10 μg (0.19 nmol) ^{89}Zr -AMG211 ($n = 6$; 5 MBq) or 10 μg (0.19 nmol) ^{89}Zr -Mec14 ($n = 6$; 5 MBq) was administered followed by microPET scanning and *ex vivo* biodistribution at 24 hours after injection.

To study CEA-dependent uptake, ^{89}Zr -AMG211 was tested in 3 groups of mice bearing tumor xenografts that expressed different levels of the CEA target. Mice bearing LS174T, BT474 or HL-60 xenografts were injected with 10 μg (0.19 nmol) of ^{89}Zr -AMG211 ($n = 6$

per group; 5 MBq). Twenty-four hours after tracer injection, mice were sacrificed for *ex vivo* biodistribution.

Half of the harvested tumors were paraffin embedded and the other half were used to make tumor lysates. Tumor lysates were obtained by homogenization with a DiAx600 (Heidolph) in RIPA buffer (Thermo Scientific) for 2-5 minutes. Blood was collected in BD Vacutainer PST Lithium Heparin Tubes (BD Biosciences) and centrifuged to collect plasma.

For all *ex vivo* biodistribution studies, tumor, whole blood, and organs of interest were collected and weighed. Samples together with tracer standards were counted in a calibrated well-type γ -counter (LKB Instruments). Uptake is expressed as % injected dose per gram of tissue (%ID/g).

The acquisition and reconstruction of microPET scans were performed as previously described (10). After reconstruction, images were interpolated using trilinear interpolation and filtered using Gaussian smoothing using AMIDE Medical Image Data Examiner software (version 1.0.4, Stanford University). Coronal microPET images were used for display. Volumes of interest (VOI) of the whole tumor were drawn based on biodistribution tumor weight. For the VOI of the heart an ellipsoid of 3x4.5x4 mm in the coronal plane was drawn. VOIs were subsequently quantified. Data are expressed as the mean standardized uptake value (SUV_{mean}).

SDS-PAGE autoradiography

Mini-PROTEANTGX Precast Gels (Bio-Rad) were loaded with 40 μg protein of tumor lysates or mouse plasma from 3 mice, tracer alone as positive control, and free ^{89}Zr -oxalate. Gels were exposed overnight to phosphor imaging screens (Perkin Elmer) in X-ray cassettes. The screens were read using a Cyclone Storage Phosphor System (Perkin Elmer) and OptiquantTM software to quantify the intensity of radioactivity. Lanes were split into regions containing intact ^{89}Zr -AMG211, high (> 80 kDa) or low molecular weight (< 40 kDa) protein associated radioactivity. Molecular weight was verified using ProSieveTM color protein maker (Lonza).

Ex vivo fluorescent imaging

For near-infrared fluorescence imaging LS174T xenograft bearing mice were co-injected with 50 (0.93 nmol), 100 (1.85 nmol) or 250 μg (4.63 nmol) of both 800CW-AMG211 and 680RD-Mec14. At 24 hours after injection, mice were sacrificed, tumor tissue was harvested, formalin-fixed and paraffin embedded. Four μm sections were incubated for 2 minutes in xylene followed by scanning 800CW-AMG211 and 680RD-Mec14 with Odyssey infrared imaging system (LI-COR Biosciences) for intratumoral distribution. After Odyssey scanning, the same tumor sections were stained with hematoxylin and eosin (H&E). In addition, subsequent tumor slices were stained with immunohistochemistry using 1 $\mu\text{g}/\text{mL}$ rabbit monoclonal CEA antibody (11077-R327; Sino Biologicals Inc.). For fluorescent microscopy, an inverted Leica DMI600B fluorescence microscope equipped with a Lumen Dynamics X-Cite 200DC light source was used. Nuclei were stained with Hoechst 33342 (Life Technologies).

CD3 binding

Binding of N-sucDf-AMG211 to T cells was assessed using a flow cytometry approach. CD3⁺ T cells were isolated from peripheral blood mononuclear cells, derived from buffy coats of healthy volunteers after informed consent (Sanquin) using Pan T-cell Isolation Kit (Miltenyi Biotec). CD3⁺ T cells (100,000) were plated with AMG 211 or N-sucDf-AMG211 (5 µg/mL) for 40 minutes at 4°C. After washing, cells were incubated with biotin labeled His-antibody (20 µg/mL; Dianova) for 30 minutes at 4°C. After another washing procedure, CD3⁺ cells were incubated with streptavidin-APC (2 µg/mL; BD Biosciences) for 20 minutes at 4°C, followed by propidium iodide staining (1 µg/mL; Thermo Fisher Scientific) to select live CD3⁺ cells. Mean fluorescence intensity of N-sucDf-AMG211 and AMG 211 bound to CD3⁺ cells was assessed by Accuri™ C6 flow cytometer (BD Biosciences) and expressed as percentage of AMG 211 binding. The assay was used as release test in manufacturing of the clinical batch of N-sucDf-AMG211.

GMP manufacturing

Manufacturing was performed according to GMP guidelines. ⁸⁹Zr-AMG211 was manufactured in a 2-step process with first the conjugation resulting after purification in the intermediate N-sucDf-AMG211, followed by the ⁸⁹Zr labeling, purification, dilution, and sterile filtration (Supplementary Fig. S1). Specifications such as conjugation ratio, purity, concentration, endotoxins, sterility, residual solvents, radiochemical purity, and immunoreactivity to both CD3 and CEA have been assessed. Stability of N-sucDf-AMG211 stored at -80°C was studied up to 6 months.

Statistical analysis

Data are presented as mean ± standard deviation (SD). Mann-Whitney U-test was performed to test differences between two groups (GraphPad, Prism 5). A Bonferroni corrected Mann-Whitney U-test was performed to compare more than two groups. To test for a dose-dependent relation, Cuzick's test for trend was used. Blood half-life was calculated using one phase decay (GraphPad, Prism 5). *P* values < 0.05 were considered significant.

Results

AMG 211 is successfully conjugated with N-sucDf and labeled with ⁸⁹Zr

The efficiency of AMG 211 conjugation was 51%. Labeling of N-sucDf-AMG211 resulted in a maximum specific activity of 500 MBq/mg with a radiochemical purity of more than 95%, with less than 5% aggregates (Supplementary Fig. S2). To prove that labeling AMG 211 did not alter the immunoreactivity towards CEA, unlabeled AMG 211 was tested in competition with ⁸⁹Zr-AMG211 batches with different chelator to AMG 211 ratios. The 2:1 conjugation ratio showed the best preserved immunoreactivity (70.7 ± 7.5% of unlabeled AMG 211) and an average IC₅₀ of 131 ± 14 nM for the competition of CEA binding with 185 nM ⁸⁹Zr-AMG211 (Supplementary Fig. S3A). As immunoreactivity decreased upon higher conjugation ratios (Supplementary Fig. S3B), a 2:1 conjugation ratio was chosen for further experiments.

⁸⁹Zr-AMG211 is internalized in CEA⁺ LS174T cells

In vitro, ⁸⁹Zr-AMG211 was internalized in LS174T cells up to 12 ± 3% of initial cell associated radioactivity at 4 hours after incubation at 37°C, whereas only 6 ± 3% was internalized at 4°C (Supplementary Fig. S4). This allows tumor accumulation over time due to residualizing capacity of ⁸⁹Zr.

⁸⁹Zr-AMG211 shows dose-dependent tumor uptake

In general, tracer uptake was highest in the kidney, indicating renal elimination, followed by tumor and liver (Fig. 1). ⁸⁹Zr-AMG211 showed an inverse protein dose-dependent tumor uptake (Fig. 1; $P_{\text{trend}} < 0.001$). ⁸⁹Zr-AMG211 uptake was relatively highest at the 2 μg dose ($7.5 \pm 1.5\% \text{ID/g}$) and lowest at the 500 μg dose ($3.9 \pm 0.13\% \text{ID/g}$). The kidneys showed a similar trend with uptake ranging from $283 \pm 34\% \text{ID/g}$ at the lowest dose and $141 \pm 33\% \text{ID/g}$ at the highest dose. Blood levels were 1%ID/g at 6 hours after injection for all dose groups. Based on sufficient tumor uptake and a maximum specific activity of 500 MBq/mg, 10 μg (5 MBq) was selected for subsequent ⁸⁹Zr-AMG211 microPET imaging studies.

⁸⁹Zr-AMG211 demonstrates specific tumor uptake in LS174T xenografts

MicroPET images revealed tumor uptake of ⁸⁹Zr-AMG211 up to 24 hours after injection, whereas the non-tumor targeting BiTE antibody construct ⁸⁹Zr-Mec14 did not show accumulation in LS174T xenografts (Fig. 2A). Tumor uptake of ⁸⁹Zr-AMG211 increased up to 6 hours after injection ($\text{SUV}_{\text{mean}} 0.64 \pm 0.10$) with prolonged retention up to at least 24 hours ($\text{SUV}_{\text{mean}} 0.61 \pm 0.06$). In contrast, tumor uptake of ⁸⁹Zr-Mec14 decreased rapidly after tracer injection (Fig. 2B), although blood levels of both tracers showed similar elimination with a circulating half-life of 0.72 hours (95% confidence interval 0.51-1.27) for ⁸⁹Zr-Mec14 and 0.96 hours (95% confidence interval 0.76 – 1.36) for ⁸⁹Zr-AMG211 (Fig. 2B). Specific tumor uptake was confirmed by *ex vivo* biodistribution analysis (Fig. 2C). Twenty-four hours after injection, ⁸⁹Zr-AMG211 tumor uptake was $6.0 \pm 1.3\% \text{ID/g}$ compared to $0.5 \pm 0.2\% \text{ID/g}$ for ⁸⁹Zr-Mec14 ($P < 0.01$). SDS-PAGE autoradiography showed intact ⁸⁹Zr-AMG211, while ⁸⁹Zr-Mec14 in LS174T xenografts lysates was absent (Fig. 2D). Both ⁸⁹Zr-AMG211 and ⁸⁹Zr-Mec14 were present intact in the plasma.

Tumor uptake of ⁸⁹Zr-AMG211 is CEA dependent

⁸⁹Zr-AMG211 was additionally studied in two other xenograft models. BT474 xenografts were used as second CEA-positive tumor model, whereas HL-60 represents CEA-negative tumor model (Supplementary Fig. S5). CEA-positive xenografts were clearly visualized with microPET up to 24 hours after injection while HL-60 tumors were not visible (Fig. 3A). Quantification of tumor uptake derived from PET images showed SUV_{mean} values between 0.5 and 0.6 for CEA-positive xenografts and below 0.2 for the CEA-negative xenografts (Fig. 3B). *Ex vivo* biodistribution confirmed image derived quantification of tumor uptake at 24 hours after injection, with highest uptake in LS174T xenografts ($6.0 \pm 1.3\% \text{ID/g}$), followed by BT474 xenografts ($3.8 \pm 1.1\% \text{ID/g}$), and lowest uptake in HL-60 xenografts ($0.45 \pm 0.05\% \text{ID/g}$; Fig. 3C). ⁸⁹Zr-AMG211 tumor uptake appeared to reflect CEA expression, with more uptake in cells expressing higher levels of CEA ($R^2 = 0.81$). SDS-

PAGE autoradiography demonstrated presence of intact ^{89}Zr -AMG211 in CEA-positive tumor lysates, whereas it was absent in CEA-negative tumor lysate (Fig. 3D), suggesting that intact ^{89}Zr -AMG211 might only be retained in the presence of cell surface tumor target.

Intratumoral ^{89}Zr -AMG211 disintegration over time

While total tumor ^{89}Zr signal remained similar at 6 and 24 hours following tracer injection, *ex vivo* tumor lysates indicated time dependent disintegration of ^{89}Zr -AMG211 in LS174T xenografts. Autoradiography showed low molecular weight species increased from $4.9 \pm 0.5\%$ at 6 hours to $47.6 \pm 3.0\%$ at 24 hours after tracer injection (Fig. 4A). In contrast, mostly intact ^{89}Zr -AMG211 was detected in the plasma samples, indicating stability of the molecule in circulation (Fig. 4B).

800CW-AMG211 localizes predominantly to viable CEA positive tumor

Intratumoral distribution was studied using fluorescently labeled AMG 211 and Mec14. A dose escalation study was performed by co-injecting 50, 100, and 250 μg of both 800CW-AMG211 and 680RD-Mec14. *Ex vivo* analysis at 24 hours after injection showed clear uptake of 800CW-AMG211 in viable CEA positive tumor areas and minor uptake in necrotic tumor tissue (Fig. 5A). No large differences in the accumulation pattern were observed between the different protein dose groups. 680RD-Mec14 was predominantly located in necrotic tumor tissue, indicating non-specific uptake. In addition, a non-specific signal was found in areas with tissue folding. Fluorescent microscopy revealed that 800CW-AMG211 is mainly located at the cellular membrane and/or in the cytoplasm and targeted less than 5% of tumor cells (Fig. 5B).

^{89}Zr -AMG211 is manufactured according to GMP guidelines

All 3 conjugation and labeling batches complied with release specifications (Supplementary Table S1), demonstrating robust manufacturing process of ^{89}Zr -AMG211. Shelf-life of intermediate N-sucDf-AMG211 has been set at 6 months at -80°C , and will, if within specifications, be extended at future time points.

The Investigational Medicinal Product Dossier (IMPD) was written, with summaries of information related to the quality, manufacture and control of the Investigation Medical Product ^{89}Zr -AMG211 included. The validation results of the three GMP batches and its stability data are also part of the IMPD. The IMPD has been approved by the competent authorities that has allowed clinical studies.

Discussion

^{89}Zr -labeled bispecific T-cell engager AMG 211 demonstrates CEA-specific tumor uptake and prolonged tumor retention up to 24 hours despite rapid elimination from the circulation. Furthermore, intact ^{89}Zr -AMG211 was found in circulation as demonstrated by SDS-PAGE autoradiography of blood samples collected from treated mice. In tumors, 800CW-AMG211 localizes to the CEA-expressing viable portion and can be found on the cell surface. Our findings indicated that ^{89}Zr -AMG211 binds specifically to CEA and stays intact in circulation *in vivo* in mouse xenograft models. ^{89}Zr -AMG211 has been produced for the

clinic using GMP compliant manufacturing, which was consistent through three validation runs.

The tumor retention of ^{89}Zr -AMG211 is remarkable. Despite low internalization of ^{89}Zr -AMG211 in LS174T cells and rapid decreasing blood levels *in vivo*, ^{89}Zr -AMG211 leads to imageable tumors for at least 24 hours after injection. Although internalization might not be useful for the mechanism of action of AMG 211, it might be the case for an imaging agent. Internalization allows tumor accumulation over time due to residualizing ^{89}Zr . For AMG 211 to induce cytotoxic T-cell mediated tumor cell killing, membrane bound intact AMG 211 is necessary, and our data confirmed that is the case. Interestingly, even though intratumoral ^{89}Zr -AMG211 was much longer retained, part of the signal was likely contributed by disintegrated ^{89}Zr -species. As a disintegrated molecule might not result in a proper immune effector function, data on intratumoral drug integrity could improve insight in functional drug exposure. Data on intratumoral drug integrity for other bispecific antibodies are currently not available, although essential for biological activity. This study demonstrates a new technique to study the intratumoral integrity of T-cell directed antibodies and derivatives. In patients treated with blinatumomab targeting CD19-positive hematological malignancies, the serum elimination half-life of blinatumomab is ~ 2 hours (13, 14). In this setting, using continuous infusion, sustainable, predictable, and dose linear drug levels in serum are achieved (13, 14). Efficacy of such an approach has been shown in non-Hodgkin and diffuse large B-cell lymphoma, indicating functional drug exposure in visceral tumor lesions (14, 15). As shown in our previous studies evaluating ^{89}Zr -AMG110 (targets CD3 and EpCAM) in mouse cancer models, prolonged tumor retention for at least 72 hours after a single intravenous injection was achieved despite a short circulating half-life similar to ^{89}Zr -AMG211 (10). Together with the current study, our data demonstrates that ^{89}Zr -BiTE antibody constructs are able to accumulate in solid tumors rapidly after intravenous administration and can be found on target expressing tumor cell surface beyond blood elimination. Our findings also suggest that a constant intravenous supply of AMG 211 should improve functional drug exposure in the tumors and perhaps lead to greater anti-tumor effects.

Using the 800CW imaging tag, AMG 211 showed to localize to CEA positive tumor cells. The low number of tumor cells targeted by 800CW-AMG211 is likely due to rapidly declining blood pools levels after a single bolus injection. To improve tumor uptake, future studies with multiple or longer infusion regimens are of interest. The localization to CEA expressing tumor tissue was also reported for a full length bispecific antibody targeting CEA and CD3 (16). In that study, CEA-expressing tumor cells (LS174T) and human peripheral blood mononuclear cells were co-cultured *in vitro* or co-grafted into immunocompromised mice. Fluorescence reflectance imaging and intravital 2-photon microscopy were employed to analyze *in vivo* tumor targeting of the labeled full length bispecific antibody, while *in vitro* confocal and intravital time-lapse imaging served to assess the mode of action of the molecule. Authors suggest that specific tumor localization was mainly through CEA targeting with only minor contributions from CD3 binding. This may be similar for AMG 211 since both therapeutics have similar equilibrium dissociation constants in the submicromolar range for CD3 and nanomolar range for CEA.

^{89}Zr -AMG211 showed uptake in both LS174T (CEA high) and BT474 (CEA low) xenografts, but not in CEA-negative HL-60 xenograft. Despite lower expression of CEA in BT474, microPET images reveal only slightly lower uptake of ^{89}Zr -AMG211 at 24 hours. Besides target expression, many aspects may play a role in drug uptake and efficacy such as perfusion, presence of stroma, tumor interstitial pressure, and anatomical location. More interestingly, *in vitro* potency of redirected lysis is similar between LS174T and BT474, despite difference in receptor expression (7). This suggests that although CEA expression is required for drug efficacy, the amount of CEA expression may not be the only factor determining anti-tumor cytotoxicity. In time, blood pool levels of ^{89}Zr -AMG211 showed no difference between the three tumor models, suggesting limited pharmacokinetic impact of potential serum CEA. This is in line with *in vitro* potency data of AMG211 showing no impact of soluble CEA antigen levels up to 5 $\mu\text{g/mL}$, simulating higher levels than typically found in serum of patients with CEA positive cancers, (7).

The field of CD3-targeting bispecific antibodies is rapidly expanding and several different formats, including BiTE constructs, dual-affinity re-targeting molecules (DART), Tandem Diabodies, and others (17) have been extensively studied in the preclinical setting. While many studies have been focused on efficacy, a few of them also addressed the interaction between drug and T cells. A bispecific antibody targeting CD3 and CEA increased T-cell infiltration in a human LS174T xenograft in a mouse model containing human peripheral blood mononuclear cells (18).

Different tumor targeting CD3 bispecific molecules may exhibit different *in vivo* properties. In a small SPECT study in five ovarian cancer patients, flow cytometry analysis indicated the binding of the bispecific F(ab')₂ targeting CD3 and the folate receptor to peripheral blood T cells (19). However, it is currently unknown whether bispecific antibody constructs like AMG 211 are first bound to circulating T cells and subsequently recruit them to the tumors, or whether the drug travels as a free agent to penetrate tumors and then induces local T-cell activation and proliferation, or both. In the current study, the impact of host effector cells could not be taken into account, since AMG 211 is not cross-reactive with mouse CD3. Progress has been made in this regard, however, modeling the human immune system in a mouse system is still far from perfect (20). Recently, a clinical study has been completed with ^{89}Zr -AMG211 (NCT02760199). In this clinical trial nine patients with relapsed/refractory gastrointestinal adenocarcinoma received ^{89}Zr -AMG211 PET scan(s) before and/or during AMG 211 treatment. Serial blood sampling and peripheral blood mononuclear cell isolation, together with PET scanning could aid in analyzing the influence of T cells on ^{89}Zr -AMG211 distribution and assist interpretation of *in vivo* mechanisms underlying tissue accumulation kinetics of the molecule.

In conclusion, this study illustrated the feasibility for using ^{89}Zr -AMG211 to assess dose-dependent CEA specific tumor uptake and tissue distribution using PET imaging. Furthermore, ^{89}Zr -AMG211 can be manufactured according to GMP guidelines. Therefore, our data enabled the use of ^{89}Zr -AMG211 in clinical trials to support further drug development.

Supplementary Material

Refer to Web version on PubMed Central for supplementary material.

Financial support

This study was supported by ERC Advanced grant OnQview provided to E.G.E de Vries and Dutch Cancer Society grant (RUG 2010 4739) provided to C.P. Schröder.

References

1. Klinger M, Benjamin J, Kischel R, Stienen S, Zugmaier G. Harnessing T cells to fight cancer with BiTE[®] antibody constructs--past developments and future directions. *Immunol Rev.* 2016; 270:193–208. [PubMed: 26864113]
2. Offner S, Hofmeister R, Romaniuk A, Kufer P, Baeuerle PA. Induction of regular cytolytic T cell synapses by bispecific single-chain antibody constructs on MHC class I-negative tumor cells. *Mol Immunol.* 2006; 43:763–71. [PubMed: 16360021]
3. Fiedler WM, Wolf M, Kebenko M, Goebeler ME, Ritter B, Quaas A, et al. A phase I study of EpCAM/CD3-bispecific antibody (MT110) in patients with advanced solid tumors. *J Clin Oncol.* 2012; 30(suppl) abstr 2504.
4. Pishvaian M, Morse MA, McDevitt J, Norton JD, Ren S, Robbie GJ, et al. Phase I dose escalation study of MEDI-565, a bispecific T-cell engager that targets human carcinoembryonic antigen, in patients with advanced gastrointestinal adenocarcinomas. *Clin Colorectal Cancer.* 2016; 15:345–51. [PubMed: 27591895]
5. Osada T, Hsu D, Hammond S, Hobeika A, Devi G, Clay TM, et al. Metastatic colorectal cancer cells from patients previously treated with chemotherapy are sensitive to T-cell killing mediated by CEA/CD3-bispecific T-cell-engaging BiTE antibody. *Br J Cancer.* 2010; 102:124–33. [PubMed: 19953093]
6. Osada T, Patel SP, Hammond SA, Osada K, Morse MA, Lyerly HK. CEA/CD3-bispecific T cell-engaging (BiTE) antibody-mediated T lymphocyte cytotoxicity maximized by inhibition of both PD1 and PD-L1. *Cancer Immunol Immunother.* 2015; 64:677–88. [PubMed: 25742933]
7. Oberst MD, Fuhrmann S, Mulgrew K, Amann M, Cheng L, Lutterbuese P, et al. CEA/CD3 bispecific antibody MEDI-565/AMG 211 activation of T cells and subsequent killing of human tumors is independent of mutations commonly found in colorectal adenocarcinomas. *MAbs.* 2014; 6:1571–84. [PubMed: 25484061]
8. Peng L, Oberst MD, Huang J, Brohawn P, Morehouse C, Lekstrom K, et al. The CEA/CD3-bispecific antibody MEDI-565 (MT111) binds a nonlinear epitope in the full-length but not a short splice variant of CEA. *PLoS One.* 2012; 7:e36412. [PubMed: 22574157]
9. Lutterbuese R, Raum T, Kischel R, Lutterbuese P, Schlereth B, Schaller E, et al. Potent control of tumor growth by CEA/CD3-bispecific single-chain antibody constructs that are not competitively inhibited by soluble CEA. *J Immunother.* 2009; 32:341–52. [PubMed: 19342971]
10. Warnders FJ, Waijjer SJ, Pool M, Lub-de Hooge MN, Friedrich M, Terwisscha van Scheltinga AG, et al. Biodistribution and PET imaging of labeled bispecific T cell-engaging antibody targeting EpCAM. *J Nucl Med.* 2016; 57:812–7. [PubMed: 26848172]
11. Verel I, Visser GW, Boellaard R, Stigter-van Walsum M, Snow GB, van Dongen GA. ⁸⁹Zr immuno-PET: Comprehensive procedures for the production of ⁸⁹Zr-labeled monoclonal antibodies. *J Nucl Med.* 2003; 44:1271–81. [PubMed: 12902418]
12. Terwisscha van Scheltinga AG, van Dam GM, Nagengast WB, Ntziachristos V, Hollema H, Herek JL, et al. Intraoperative near-infrared fluorescence tumor imaging with vascular endothelial growth factor and human epidermal growth factor receptor 2 targeting antibodies. *J Nucl Med.* 2011; 52:1778–85. [PubMed: 21990576]
13. Zhu M, Wu B, Brandl C, Johnson J, Wolf A, Chow A, et al. Blinatumomab, a bispecific T-cell engager (BiTE[®]) for CD-19 targeted cancer immunotherapy: Clinical pharmacology and its implications. *Clin Pharmacokinet.* 2016; 55:1271–88. [PubMed: 27209293]

14. Goebeler ME, Knop S, Viardot A, Kufer P, Topp MS, Einsele H, et al. Bispecific T-cell engager (BiTE) antibody construct blinatumomab for the treatment of patients with relapsed/refractory non-Hodgkin lymphoma: Final results from a phase I study. *J Clin Oncol*. 2016; 34:1104–11. [PubMed: 26884582]
15. Viardot A, Goebeler ME, Hess G, Neumann S, Pfreundschuh M, Adrian N, et al. Phase 2 study of the bispecific T-cell engager (BiTE) antibody blinatumomab in relapsed/refractory diffuse large B-cell lymphoma. *Blood*. 2016; 127:1410–6. [PubMed: 26755709]
16. Lehmann S, Perera R, Grimm HP, Sam J, Colombetti S, Fauti T, et al. In vivo fluorescence imaging of the activity of CEA TCB, a novel T-cell bispecific antibody, reveals highly specific tumor targeting and fast induction of T-cell-mediated tumor killing. *Clin Cancer Res*. 2016; 22:4417–27. [PubMed: 27117182]
17. Zhukovsky EA, Morse RJ, Maus MV. Bispecific antibodies and CARs: Generalized immunotherapeutics harnessing T cell redirection. *Curr Opin Immunol*. 2016; 40:24–35. [PubMed: 26963133]
18. Bacac M, Fauti T, Sam J, Colombetti S, Weinzierl T, Ouaret D, et al. A novel carcinoembryonic antigen T-cell bispecific antibody (CEA TCB) for the treatment of solid tumors. *Clin Cancer Res*. 2016; 22:3286–97. [PubMed: 26861458]
19. Tibben JG, Boerman OC, Massuger LF, Schijf CP, Claessens RA, Corstens FH. Pharmacokinetics, biodistribution and biological effects of intravenously administered bispecific monoclonal antibody OC/TR F(ab')₂ in ovarian carcinoma patients. *Int J Cancer*. 1996; 66:477–83. [PubMed: 8635863]
20. Zitvogel L, Pitt JM, Daillere R, Smyth MJ, Kroemer G. Mouse models in oncoimmunology. *Nat Rev Cancer*. 2016; 16:759–73. [PubMed: 27687979]

Translational Relevance

Approval of the CD19 and CD3 targeting bispecific T-cell engager (BiTE) antibody construct, blinatumomab, for treating relapsed and refractory B-cell precursor acute lymphoblastic leukemia patients clearly demonstrated that tumor targeted immunity is an effective approach. BiTE[®] antibody constructs induced tumor cell killing independent of antigen specificity or costimulatory factors by connecting cancer cells to cytotoxic T cells. While this approach has offered significant clinical benefits in hematologic malignancy, recent exploration have also been focused on solid tumors.

This study provides non-invasive molecular imaging insight into solid tumor targeting and biodistribution of the carcinoembryonic antigen (CEA) and CD3 targeting BiTE antibody construct AMG 211 in preclinical mouse xenograft models. ⁸⁹Zr-AMG211 PET-imaging showed dose-dependent accumulation in CEA-expressing tumors. Although ⁸⁹Zr-AMG211 circulating blood half-life was ~1, hour, the signal persisted in tumors for up to 24 hours. Good Manufacturing Practice compliant ⁸⁹Zr-AMG211 was produced and evaluated in a recently completed clinical trial (NCT02760199).

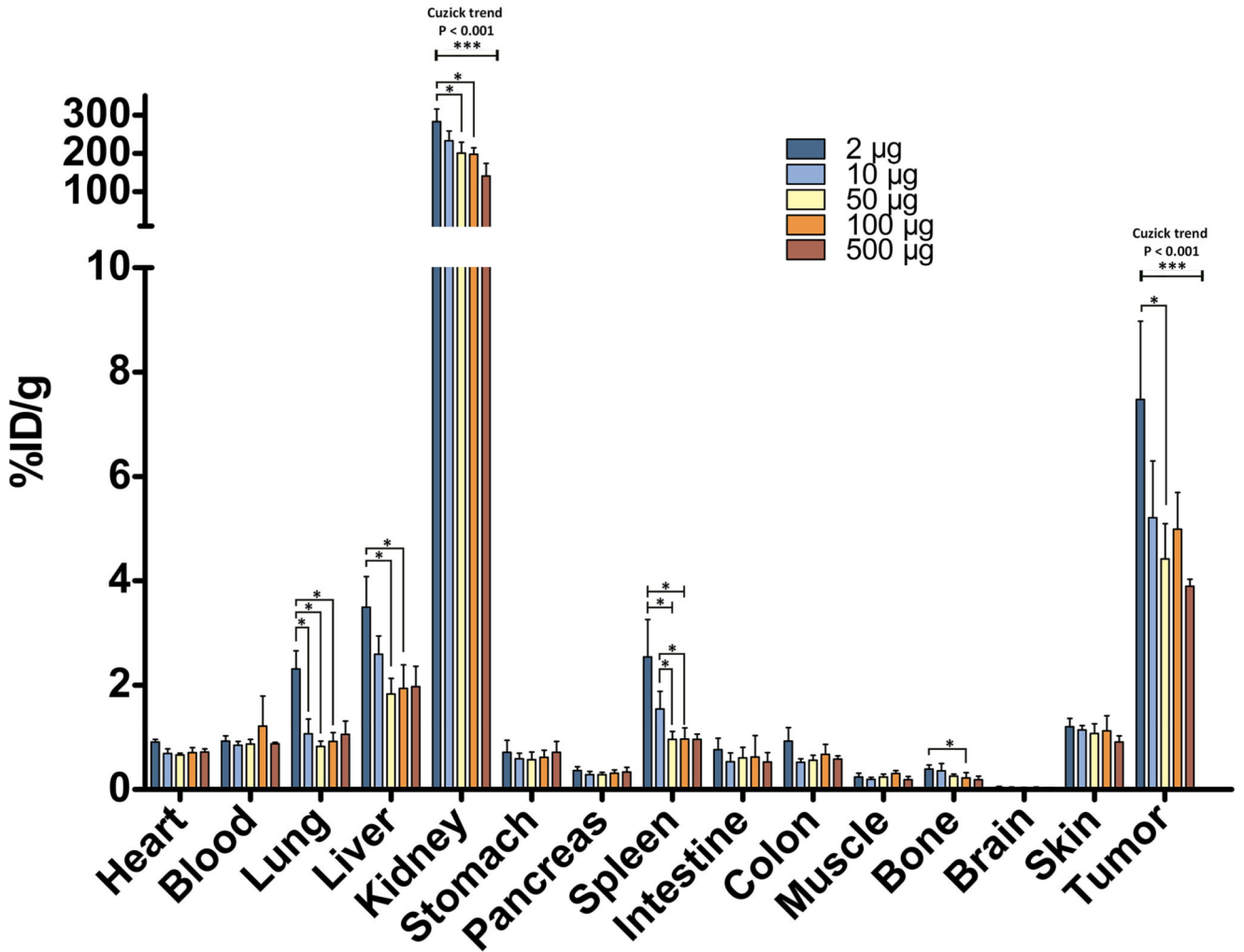


Fig. 1. Dose dependent ^{89}Zr -AMG211 biodistribution in LS174T-tumor bearing mice at 6 hours post injection. Mice were injected with 2 ($n = 6$), 10 ($n = 6$), 50 ($n = 6$), 100 ($n = 6$) or 500 μg ($n = 3$) protein doses. Data are mean \pm SD. * $P < 0.05$; *** $P < 0.001$.

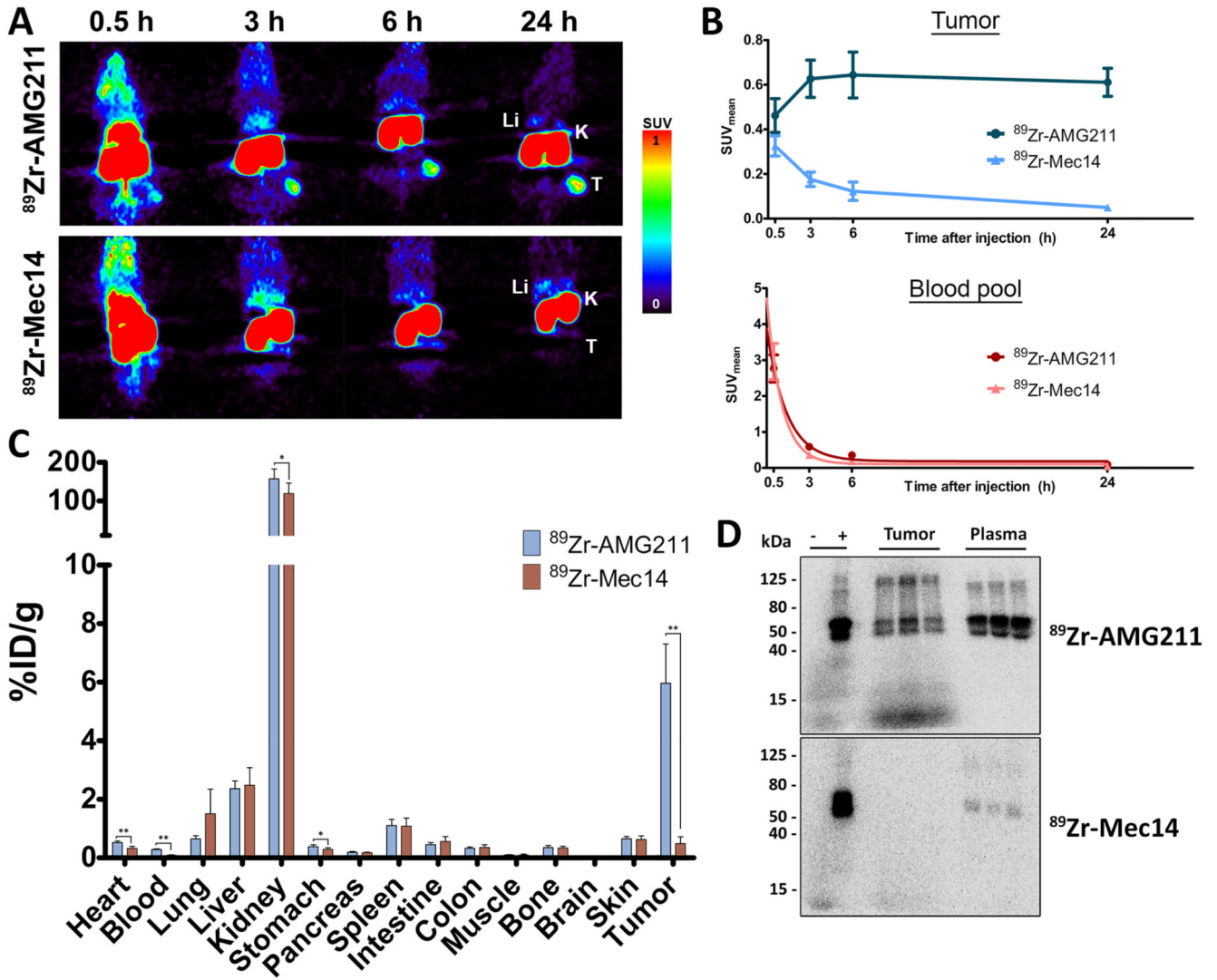


Fig. 2. Specific tumor uptake of ^{89}Zr -AMG211 in LS174T tumor bearing mice. **A)** Representative coronal small-animal PET images up to 24 h after injection of $10\ \mu\text{g}$ ^{89}Zr -AMG211 ($n = 6$) or ^{89}Zr -Mec14 ($n = 6$). Li = liver; K = kidney; T = tumor. **B)** Image quantification of LS174T tumors (upper panel) and blood pool (lower panel). *Ex vivo* **C)** biodistribution and **D)** SDS-PAGE autoradiography ^{89}Zr -AMG211 and ^{89}Zr -Mec14 24 hours after injection. + : ^{89}Zr -tracer prior to injection; - : free ^{89}Zr only; tumor: lysates of 3 different LS174T xenografts; plasma: plasma samples from corresponding mice. Data are mean \pm SD. * $P < 0.05$; ** $P < 0.01$.

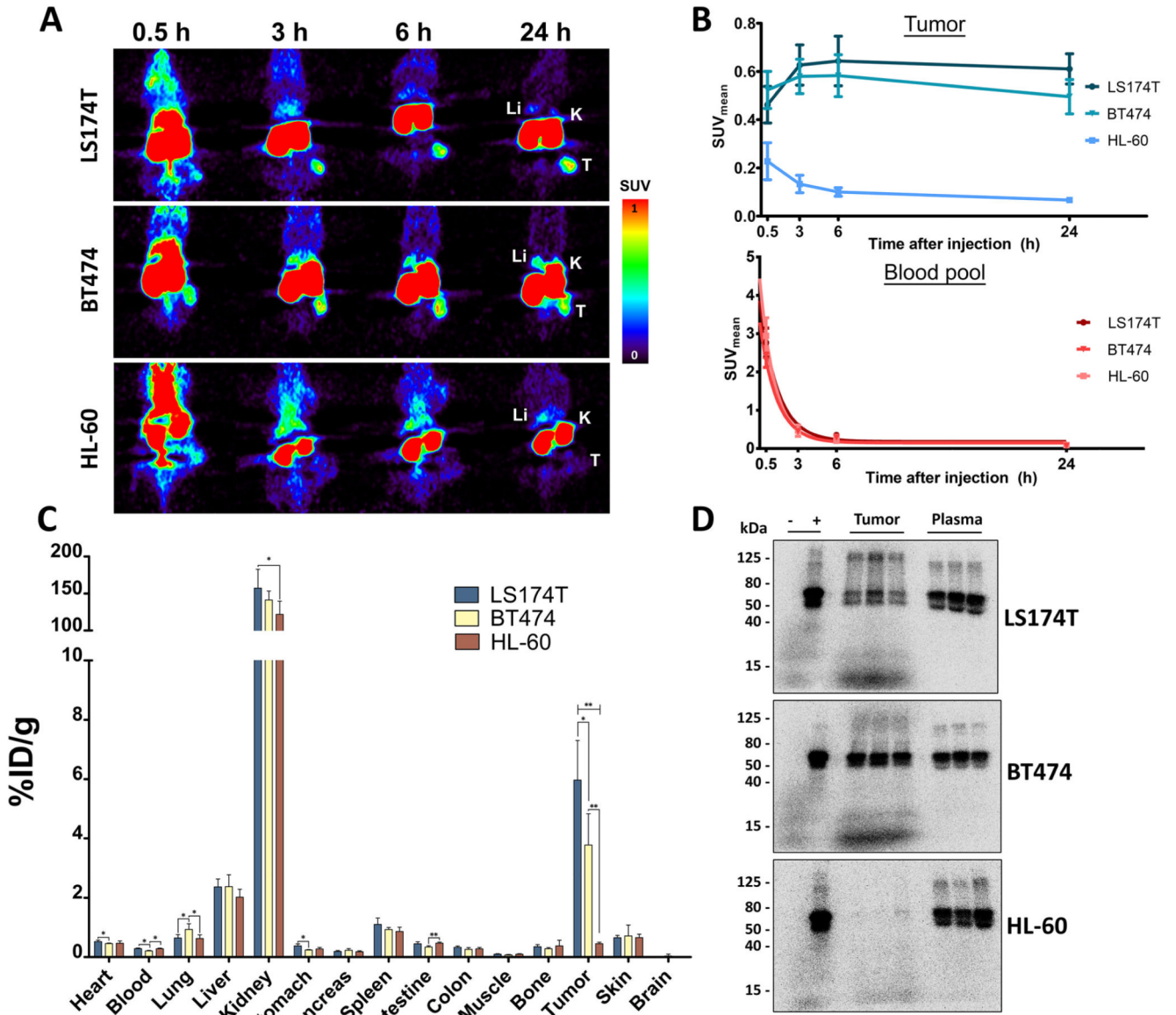


Fig. 3. Uptake of ^{89}Zr -AMG211 in LS174T ($n = 6$), BT474 ($n = 6$) or HL-60 ($n = 6$) tumor bearing mice. A) Representative coronal small-animal PET images up to 24 hours after injection of $10\ \mu\text{g}$ ^{89}Zr -AMG211. Li = liver; K = kidney; T = tumor. B) Quantification of tumors (upper panel) and blood pool (lower panel). *Ex vivo* C) biodistribution and D) SDS-PAGE autoradiography ^{89}Zr -AMG211 24 hours after injection. + : ^{89}Zr -AMG211 prior to injection; - : free ^{89}Zr only; tumor: lysates of 3 different tumor bearing mice; plasma: plasma samples from corresponding mice. Data are mean \pm SD. * $P < 0.05$; ** $P < 0.01$.

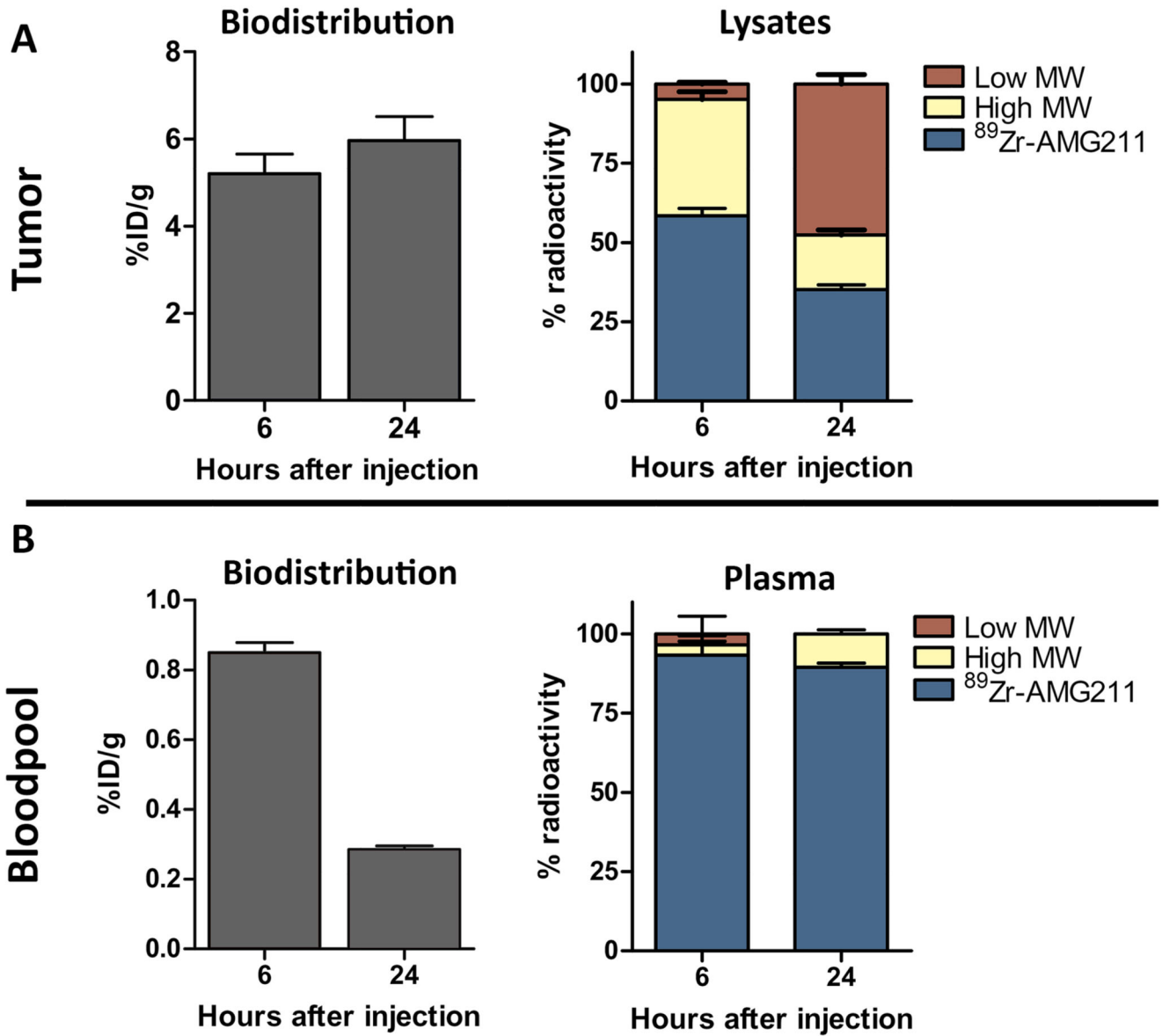


Fig. 4. Change in integrity of ^{89}Zr -AMG211 in tumor over time. A) Absolute uptake of ^{89}Zr -AMG211 in LS174T xenografts (left panel) and integrity of ^{89}Zr -AMG211 in LS174T lysates (right panel) at 6 and 24 hours after injection. B) Uptake of ^{89}Zr -AMG211 in blood (left panel) and integrity of ^{89}Zr -AMG211 in plasma (right panel) at 6 and 24 hours after injection. MW = molecular weight. Data are mean \pm SD.

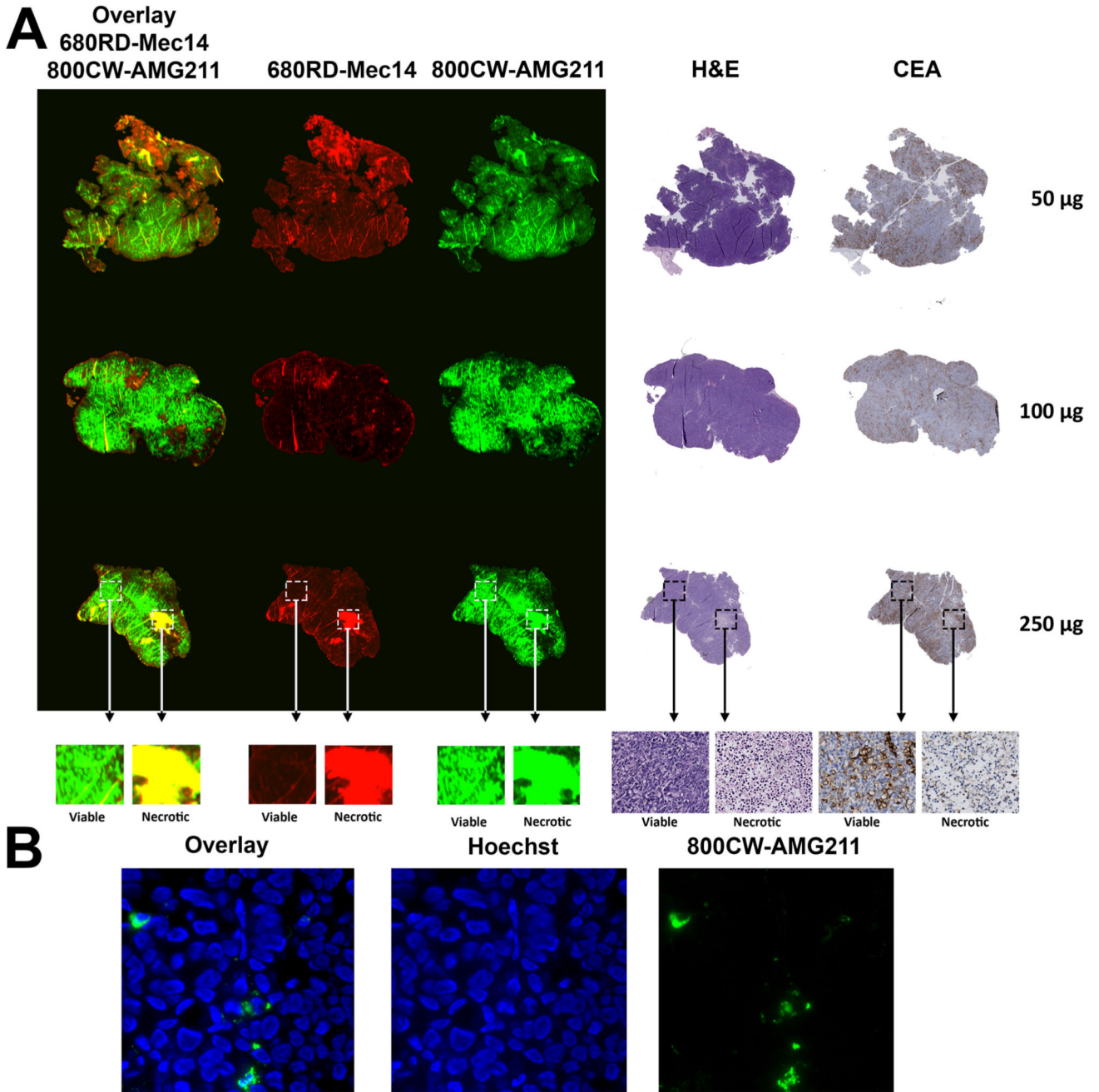


Fig. 5. Intratumoral distribution of escalating doses of co-injected 800CW-AMG211 and 680RD-Mec14 (50, 100 or 250 µg) in LS174T tumors. (A) Macroscopic fluorescent imaging of 800CW-AMG211 (green) and 680RD-Mec14 (red) distribution, with overlapping signal (yellow) in necrotic tissue as visualized by hematoxylin and eosin (H&E). 800CW-AMG211 mainly localizes to viable tissue according to H&E with concordant CEA immunohistochemical staining. (B) Fluorescence microscopy images (630×), visualizing

membrane and/or cytoplasmic localization of 800CW-AMG211 (green) and Hoechst stained nuclei (blue).